



Influence of the antiseptic octenidine on spectral characteristics and energy migration processes in photosystem II core complexes

Vladimir Z. Paschenko¹ · Eugene P. Lukashev¹ · Mahir D. Mamedov² · Boris N. Korvatovskiy¹ · Peter P. Knox¹

Received: 3 July 2022 / Accepted: 29 September 2022 / Published online: 5 November 2022
© The Author(s), under exclusive licence to Springer Nature B.V. 2022

Abstract

Herein, the effect of cationic antiseptics (chlorhexidine, picloxadine, miramistin, octenidine) on the initial processes of the delivery of light energy and its efficient use by the reaction centers in intact spinach photosystem II core complexes has been investigated. The characteristic effects—an increase in the fluorescence yield of light-harvesting pigments and a slowdown in the rate of energy migration in bacterial photosynthetic chromatophores has been recently demonstrated mainly in the presence of octenidine (Strakhovskaya et al., in *Photosynth Res* 147:197–209, 2021; Knox et al., in *Photosynth Res*, <https://doi.org/10.1007/s11120-022-00909-8>, 2022). In this study, we also observed that in the presence of octenidine, the fluorescence intensity of photosystem II core complexes increases by 5–10 times, and the rate of energy migration from antennae to the reaction centers decreases by 3 times. In addition, with an increase in the concentration of this antiseptic, a new effect related to a shift of the spectrum, absorption and fluorescence to the short-wavelength region has been found. Similar effects were observed when detergent Triton X-100 was added to photosystem II samples. We concluded that the antiseptic primarily affects the structure of the internal light-harvesting antenna (CP43 and CP47), through which the excitation energy is delivered to the reaction center. As a result of such an impact, the chlorophyll molecules in this structure are destabilized and their optical and functional characteristics change.

Keywords Photosystem II · Light-harvesting complexes · Energy transfer · Cationic antiseptics

Introduction

The influence of a number of cationic antiseptics (chlorhexidine, picloxadine, miramistin, octenidine) in the range of micromolar concentrations on the light-harvesting function and the delivery of light excitation energy has been recently studied in antenna complexes of bacterial photosynthetic membranes of *Rhodobacter (Rba.) sphaeroides* and *Rhodospirillum rubrum* (Strakhovskaya et al. 2021; Knox et al. 2022). Interest in such works is explained, in particular, by the fact that the accumulation of organic compounds in the global ocean, soils, and sediments can adversely affect

the biosphere. Moreover, the total use of antiseptics may also be related to the spread of the coronavirus pandemic. We found that in purple bacteria, antiseptics decoupled the processes of light energy delivery both from the peripheral light-harvesting LH2 to the LH1-reaction center (RC) core complex and within the core complex to the photoactive pigment. In this regard, it seems important to continue this line of research and to investigate the effect of these compounds on pigment-protein complex of photosystem II (PSII) from oxygenic photosynthetic organisms.

Virtually all life of higher form is dependent on oxygen, whereas plants, algae, and cyanobacteria produce most of the atmospheric oxygen on our planet. PSII, a large pigment–protein complex embedded in the thylakoid membranes of chloroplasts and cyanobacteria uses light energy to drive two chemical reactions: the oxidation of water to molecular oxygen and the reduction of plastoquinone to plastohydroquinone (reviewed in Wydrzynski and Satoh 2005; Kern and Renger 2007; Lubitz et al. 2019). PS II consists of more than 20 polypeptides and a number of cofactors associated with the electron-transfer chain (Guskov et al.

✉ Peter P. Knox
knox@biophys.msu.ru

¹ Biophysical Department, Faculty of Biology,
M.V.Lomonosov Moscow State University, Leninskiye Gory
1, Build. 12, Moscow, Russia 119234

² A.N.Belozersky Institute of Physico-Chemical Biology,
Moscow State University, Leninskiye Gory 1, Build. 40,
Moscow, Russia 119992

2009; Umena et al. 2011; Suga et al. 2015; Wei et al. 2016). The minimal protein ensemble capable of light-driven oxidation of water and reduction of plastoquinone molecule(s) consists of a Mn_4CaO_5 cluster, two integral antenna proteins CP43 and CP47, a photosynthetic reaction center (RC) containing D1, D2, and *cytb₅₅₉* subunits, and a peripheral protein PsbO (manganese-stabilizing protein) is called the PSII core complex. The PSII RC complex forms a dimer, where each monomer contains the redox-active cofactors (6 chlorophylls *a*, 2 pheophytins, 2 plastoquinones, and a non-heme iron) coordinated by D1/D2 proteins. The CP43 antenna protein binds less strongly to the D1/D2 heterodimer of the RC than CP47 and, possibly, is involved in the stabilization of the water oxidation complex. In turn, in addition to energy transfer, CP47 also seems to play a certain structural role, promoting close association of D1 and D2 subunits.

In the red region, the absorption spectra of CP47 at cryogenic temperatures have a complex structure (at least 2 components), which probably reflects the presence of chlorophyll (Chl) *a* molecules in different environments within the complex. Fluorescence for the lowest energy state (at ~685 nm) occurs at 690 nm. Since this state is lower in energy than photoactive pigment P_{680} , it may be a trap for a significant part of the excitations in CP47 or PSII core complexes (Groot et al. 1995).

The presence of 2 “red” states in the Q_Y absorption band of Chl at 4 K was also revealed in the CP43 complex from spinach: a very narrow (~2.7 nm) band at 682.5 nm has the oscillatory strength of one Chl *a* molecule, and a much broader band at 679 nm which is associated with several excitonically interacting Chl molecules (Groot et al. 1999). CP47 is located in the central part of the PSII-LHCII supercomplex and, apparently, plays a role in the dimerization of the PSII core complex, while the CP43 complex has a more peripheral localization and probably transfers the excitation energy from the peripheral antenna to the RC. Two redshifted Chl *a* spectra with fluorescence peaks at 685 and 695 nm are specifically attributed to the Chl-45 or Chl-43 molecules in CP43 and the Chl-29 molecule in CP47, respectively (Loll et al. 2005). It has been suggested that Chl-29, which is involved in the transfer of excitation energy from the peripheral antenna, can also be involved in the processes of photoprotection under light stress (Shibata et al. 2013).

It has been shown that isolated CP47 complex at cryogenic temperatures has three distinct fluorescence bands: 695 (F1), 691 (FT1), and 685 nm (FT2) (Neupane et al. 2010). In doing so, the last two peaks are attributed to the luminescence of partially destabilized Chl-protein complexes. The chlorophylls in CP47 core antenna complex of PSII are linked via efficient energy transfer to the lowest

energy trap at 695 nm (Neupane et al. 2010). In contrast to CP43, a higher sensitivity to destabilization was found for the CP47 subunit; however, the extremely sensitive nature of its relationship between protein conformation and electronic spectra is retained even when CP47 complexes are stored in the absence of glass forming agents such as glycerol and ethylene glycol. The sensitivity of these complexes may be the reason for significant variations in their optical spectra at cryogenic temperatures for different samples; minor changes in the protein environment of chlorophylls are immediately reflected in the low-temperature spectra of preparations. The presence of structurally different pools of Chl molecules in CP47 and the role of chromophore-protein interactions in the mechanism of energy transfer in the 47-kD antenna protein and its complex with the PSII RC core are reported earlier (de Paula et al. 1994). Thus, fluorescence kinetic measurements ($\lambda_{\text{ex}} = 620 \text{ nm}$, $f = 3.8 \text{ MHz}$) reveal three main components in these complexes with lifetimes of ~0.07 ns, 0.3–0.5 ns, and ~3 ns. However, after treatment of the PSIIcore/CP47 complexes with 0.2% Triton X-100, the fluorescence kinetics significantly slows down: the component with $\tau \sim 0.07 \text{ ns}$ completely disappears, and the component characterized by a fluorescence lifetime of more than 5 ns becomes dominant. It has been suggested that the slowing down of the kinetics is due to structural perturbation of protein-pigment complexes by TritonX-100 under maintaining “suboptimal interchromophoric bond” in them. As a result, the processes of energy migration slow down and the stabilization of light-induced charge separation in the RC is disturbed.

Numerous variations in the lifetime and fluorescence kinetic components found in the case of isolated PSII protein-pigment complexes can be associated by structurally heterogeneous samples (de Paula et al. 1994). According to (Hansson et al. 1988), the action of a detergent can also affect the coupling between the RC and the light-harvesting antenna, thereby changing the rate of excitation energy migration in the RC. In addition, the amount of active reaction centers with charge separation between the primary electron donor (P_{680}) and pheophytin (Pheo) can change. This is due to a change in the equilibrium between the radical ion pair $\text{P}_{680}^+\text{Pheo}^-$ and the excited states of antenna Chl, which causes the appearance of additional ways of deactivating the excitation energy. It is interesting that the reduction of the primary quinone acceptor Q_A can also lead to a similar result due to the effect of the electric charge on the electron transfer rate from P_{680}^* to Pheo (Hansson et al. 1988). According to (Schatz et al. 1988), Q_A reduction in PSII RCs controls both the yield of radical pair formation (in closed RCs, the charge photoseparation rate constant

decreases by ~6 times) and the exciton lifetime of antenna Chl *a*. At the same time, in the closed RCs, the number of light-induced primary radical pairs should also be significantly decreased.

In this study, we investigated the possible effect of a number of cationic antiseptics on the initial processes of light energy delivery and its efficient use by the reaction centers in intact spinach PSII core complexes.

Materials and methods

Isolation and purification of PSII core complexes

The oxygen-evolving PSII core complexes were isolated from fresh spinach plants (*Spinacia oleracea*) (Haag et al. 1990) by treatment of the membrane fragments with n-dodecyl β -D-maltoside (10:1, detergent/chlorophyll) for 1 h followed by sucrose density centrifugation (20–40%) for 7 h at 210,000 $\times g$ using a Beckman VTi 50 vertical rotor. The total Chl concentration of the PSII samples (~2.7 mg Chl mL⁻¹) were determined by the method described in (Porra et al. 1989). Storage/assay medium contained 25 mM Mes-NaOH (pH 6.5), 15 mM NaCl, 5 mM CaCl₂, 0.03% (w/v) n-dodecyl- β -D-maltoside. Oxygen-evolving PSII core complexes extracted from spinach practically do not contain light-harvesting complex II (LHCII) (Haag et al. 1990).

The oxygen-evolving activity (1500–1600 $\mu\text{mol O}_2 \cdot (\text{mg Chl})^{-1} \text{h}^{-1}$) of PSII complexes in the presence of 0.1 mM of DCBQ and 1.0 mM of potassium ferricyanide under continuous saturating illumination was monitored through the detection of dissolved O₂ using a Clark-type electrode.

Spectral and kinetics measurements

Ready-made pharmaceutical preparations chlorhexidine bidigluconate 20% (22.2 mM), picloxydine dihydrochloride 0.05% (1 mM), miramistin 0.01% (0.22 mM), and octenidine 0.1% (1.5 mM) were added to 1 ml PSII suspension in 25 mM MES buffer (pH 6.5) in 1 \times 1 cm quartz glass cuvette. The optical density of the sample did not exceed 0.2 OD at the absorbance maximum at ~670 nm. All antiseptics, with the exception of octenidine, were dissolved in pure water. Octenidine (marketed under the name of Octenisept) was in a form of octenidine dihydrochloride in water solution with 2% phenoxyethanol. The last one is the organic compound with the formula C₆H₅OC₂H₄OH. It is a colorless oily liquid, classified as a glycol ether, and commonly used as a preservative in vaccine formulations. In special control experiments, we added the pure phenoxyethanol water solution in one order high concentration and no effect was found

on either the absorbance spectra or the fluorescence spectra of PSII core complexes.

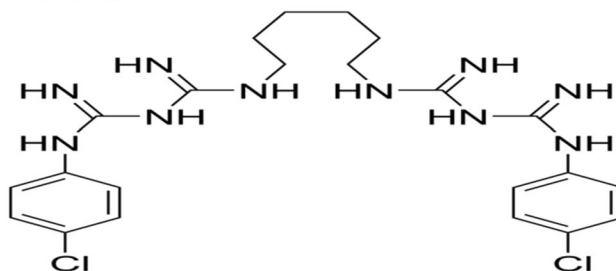
All antiseptics solutions are transparent to visible light, and in this spectral range (400–800 nm) they have neither absorption bands nor fluorescence bands. Thus, all recorded changes in the optical properties of PSII are determined by the specific effect of antiseptics on the pigment apparatus of these particles.

The measurements were performed at room temperature (22 \pm 1 °C) after 5 min of incubation.

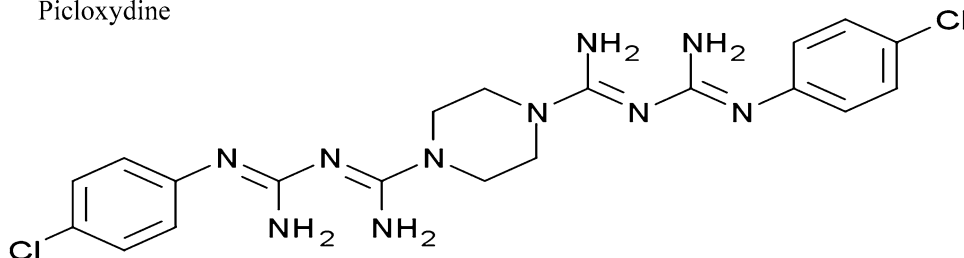
Absorption spectra were recorded with a modified Hitachi-557 spectrophotometer; Fluorescence spectra were detected using a Horiba-Jobin-Yvon Fluorolog-3 spectrofluorimeter equipped with high sensitive IR photomultiplier Hamamatsu 5509-72. Fluorescence spectra were recorded with excitation at 400 nm. The bandwidth was 10 nm for excitation light and 5 nm for emission light. The fluorescence decay kinetic curves were measured at the maximum of PSII core complexes fluorescence band (680 nm) using Becker & Hickl time correlated single photon counting system (TCSPC) with extremely high dynamic hybrid photodetector HPM-100-07. A Tema-150 femtosecond laser system (Avesta-Project LLC, Russia) was used as a source of exciting light. It generated 300-fs light pulses at 400 nm (repetition frequency, 80 MHz; average radiation power, 2.8 W; single pulse energy, 34 nJ). In the experiments, the energy of the exciting light pulses was reduced using neutral light filters to a level determined by the sensitivity of the recording system. The average radiation power density was 3 \times 10⁻⁴ W/cm². The fluorescence kinetics was approximated using the three-exponential fitting. The decay times τ were calculated using the least-squares fitting algorithm taking into account the instrumental response function (IRF) with FWHM \approx 16 ps. The measurements were repeated three times, and the mean values with standard error were used to calculate lifetime (τ) and yield (F) of fluorescence. All calculation and drawing were performed using the Origin 8.1 software (OriginLab, USA).

The structures of cationic antiseptics are shown below.

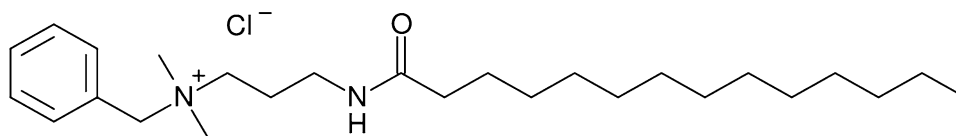
Chlorhexidine



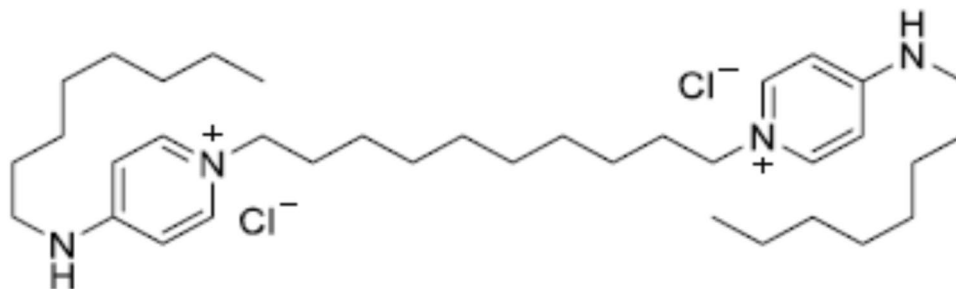
Picloxydine



Miramistin



Octenidine dihydrochloride



All studied antiseptics are colorless, that is, they do not have absorption bands in the visible region of the spectrum. We demonstrate below in the figure the absorption spectra of PSII in the control and in the presence of octenidine, which shows that additional absorption bands do not appear. These compounds also do not fluoresce in the studied wavelength range. Thus, it can be concluded that the observed changes in the fluorescence yield and chlorophyll lifetime are not affected by any intrinsic optical changes of the antiseptics.

Results

The antiseptics we use differ in their chemical structure and ability for electrostatic interactions. Accordingly, the effectiveness of their influence on the spectral characteristics and

processes of energy migration in the membranes of purple bacteria also differs (Strakhovskaya et al. 2021; Knox et al. 2022). Studying the effect of these four antiseptics on the PSII core complex shows that the characteristic effect—an increase in the fluorescence yield of light-harvesting pigments, previously found on bacterial membrane preparations, is clearly manifested only in the presence of octenidine (Fig. 1). Adding miramistin caused a very weak effect, while chlorhexidine and picloxydine even decreased the fluorescence yield. Figure 1 shows the areas under the fluorescence spectra of PSII core complexes containing 100 μM picloxydine, chlorhexidine, octenidine, and miramistin compared with the fluorescence of control preparations. The area under the fluorescence curve in the control was taken equal to unity. Insignificant quenching of fluorescence by picloxydine and chlorhexidine relative to the control was

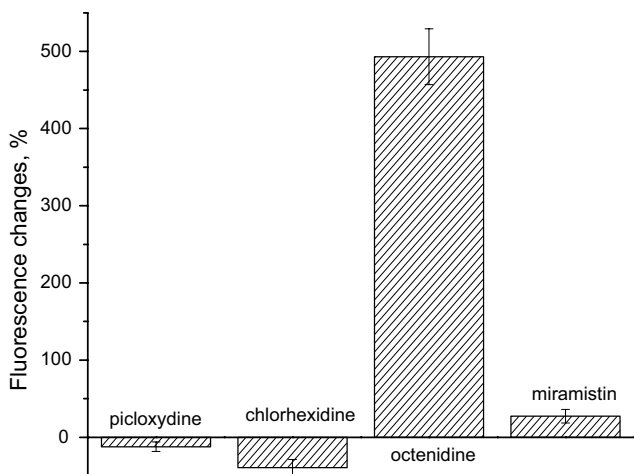


Fig. 1 Integral area of the main fluorescence band at 685 nm in PSII core complexes upon addition of 100 μM chlorhexidine, picloxydine, miramistin, and octenidine as compared with the fluorescence of the control sample (the area under the fluorescence curve for the control preparation was taken as unity). The measurements were repeated three times. The bar shows the standard deviation from mean value

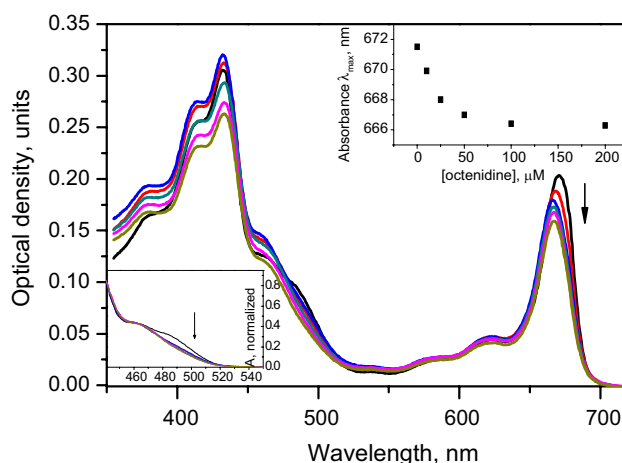
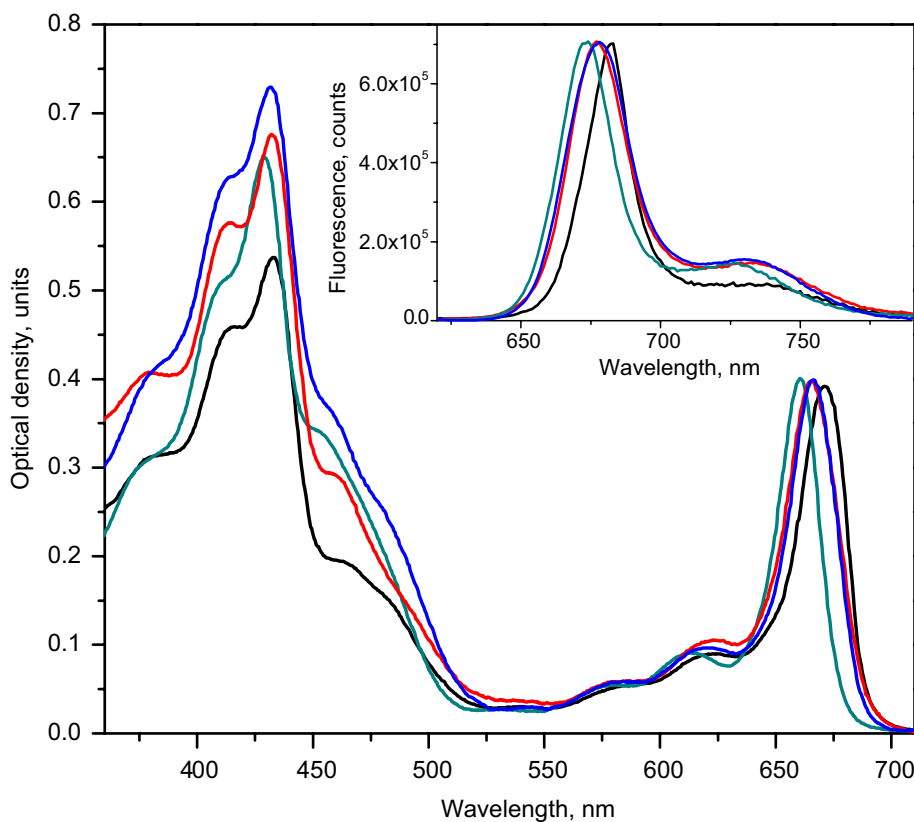


Fig. 3 Changes in absorption spectra of PSII core complexes in the presence of octenidine. The arrow in the figure shows the direction of change in the spectra upon the successive addition of octenidine at concentrations of 25, 50, 100, 200, and 300 μM . The right inset shows the position of the maximum of the Q_y absorption band in the presence of octenidine, the left inset—the change in absorption in the blue spectral region corrected for the effect of light scattering

also accompanied by a slight decrease in the optical density in the 350–700 nm spectral range (data not shown). This probably occurs as a result of the destructive effect of these

agents on the structure of chlorophyll molecules, leading to the degradation of some of their fraction.

Fig. 2 Normalized absorption and fluorescence spectra (inset) of PSII core complexes. Control sample (black curves), in the presence of 300 μM octenidine (red curves), in the presence of 0.3% (w/v) Triton X-100 (blue curves) and 80% acetone (green curves)



The following experiments were conducted to investigate in detail the effect of octenidine on the spectral and functional characteristics of PSII. An increase in the fluorescence yield in the samples upon the addition of octenidine is accompanied by a short-wavelength shift of both the absorption maximum, from 672 to 666 nm, and the fluorescence maximum, from 682 to 678 nm. A similar shift of the fluorescence band also occurs in the presence of the detergent Triton X-100. Therefore, we compared the effect of these two different agents on the spectral and kinetic characteristics of PSII core complexes.

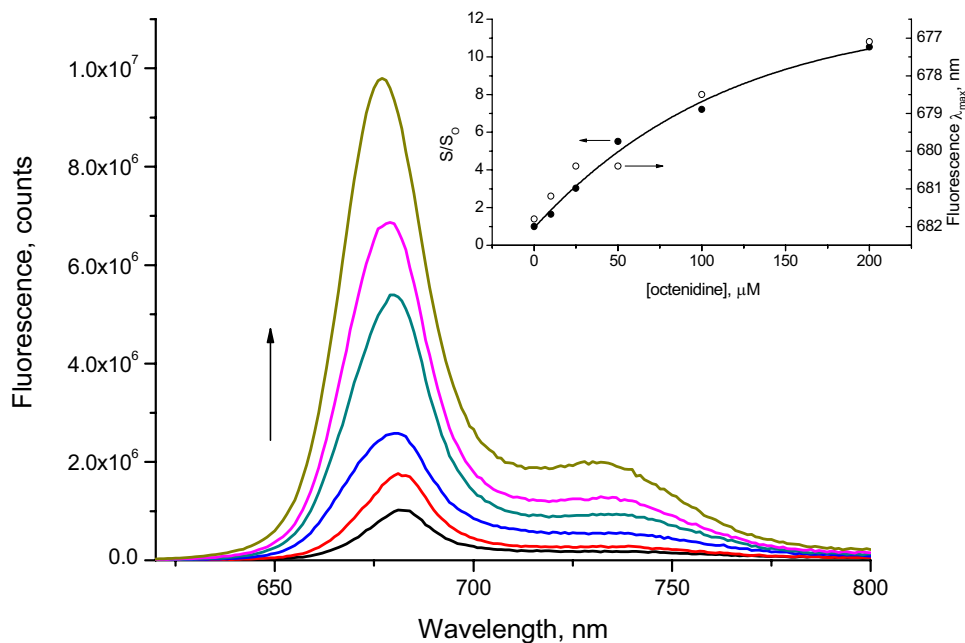
The normalized absorption and fluorescence spectra for the PSII control preparation, the spectra of samples treated by octenidine and Triton X-100, as well as the spectrum of pigments extracted from the protein complex by acetone (actually a solution of monomeric Chl) are shown in Fig. 2. It can be seen that in the case of the acetone extract, the absorption band in the red region and the fluorescence band are shifted much more strongly compared to the control sample; the absorption maximum shifts to 661 nm, and the fluorescence maximum—to 673 nm. Thus, although the treatment of PSII core complexes at maximum concentrations of octenidine and Triton X-100 leads to structural disturbances of pigment-protein complexes, ‘suboptimal interchromophore bonds’ are preserved. This is correlated with the conclusion made by de Paula et al. (1994) about the effect of the Triton X-100 on CP47 antenna / PSII core complexes. It should be noted here that the details of the interaction of the charged octenidine molecule and the neutral Triton X-100 molecule on the biostructures obviously differ. But due to the amphipathic nature of the octenidine molecule, its interaction with biostructures that have both

polar and hydrophobic regions can have a “detergent-like manner” (Malanovic et al. 2020).

The effect of increasing concentrations of octenidine on the absorption spectra of PSII core complexes is shown in Fig. 3. It can be seen that the most pronounced alterations in these spectra are due to a change in the absorption intensity of the long-wavelength component Q_y of the Chl *a* absorption band at 670 nm and in the Soret band; with an increase in the concentration of octenidine, the position of the absorption peak shifts to the short-wavelength region from 672 to 666 nm. A noticeable increase in absorption in the Soret region is most likely due to a change in the scattering of particles due to their aggregation in the presence of octenidine. A similar turbidity of the suspension, visible even to the naked eye, was observed earlier in experiments with bacterial chromatophores.

According to Shan et al. (2001), Chl *a* molecules in spinach CP43 and CP47 antenna complexes are in two spectrally different forms with long-wavelength (about 680 nm) and short-wavelength (about 670 nm) absorption maxima. It has been suggested that the presence of two spectral forms in the Q_y absorption band is due to differences in their microenvironment, as well as differences in their packaging in the protein carrier. The long-wavelength forms are possibly formed by spatially closer Chl molecules. These two spectral forms also differ in their sensitivity to external factors. Thus, the sensitivity of the long-wavelength form of Chl to heating can shift its absorption maximum to the short-wavelength region. The temperature factor, acting on the protein carrier, disrupts the initial exciton interaction of long-wave chlorophylls, which leads to the observed short-wave shift of their absorption maximum (Shan et al. 2001).

Fig. 4 Effect of octenidine on the fluorescence spectra of PSII core complexes. The arrow indicates the direction of change in the spectra derived from the control sample (black curve) with the sequential addition of 10, 25, 50, 100, and 200 μM octenidine. The inset shows the dependence of the position of the maximum of the fluorescence spectrum and the fluorescence quantum yield, determined by the ratio of the areas under the fluorescence curve on the concentration of octenidine. S/S_0 is the area under the fluorescence curve of the control preparation



Obviously, octenidine, penetrating into the structure of light-harvesting proteins, can lead to a similar effect.

Note that under the influence of an antiseptic, a certain pheophytinization of the samples (the transformation of a part of the Chl *a* molecules into Pheo *a*) can probably occur. According to Wang et al. (2020), a characteristic difference between the absorption of Chl and Pheo in the blue-green region of the spectrum is the absence of absorption at 440–500 nm in the case of Pheo. Indeed, taking into account the contribution of light scattering when normalizing the absorption spectra of PSII preparations in the presence of octenidine, a decrease in extinction in this region of the spectrum is occurred even at an octenidine concentration of about 25 μM (inset of Fig. 3).

In favor of the possible pheophytinization effect, it can also be noted that the acetone extract of our PSII preparations is characterized by the main fluorescence maximum at 673 nm (inset of Fig. 2), which coincides with the Pheo *a* fluorescence maximum in an organic solvent (ether) (French et al. 1956). For Chl *a* in ether and acetone, the position of this maximum is 668 and 669 nm, respectively. At the same time, it is quite probable that in our case this fluorescence can be associated with the denaturation products of the Chl-containing proteins. Note that the effect of pheophytinization with the addition of the antiseptics was previously argued in more detail when studying the effects of antiseptics on the purple photosynthetic bacterial membranes (Strakhovskaya et al. 2021). In this case, the fluorescence of BPheo molecules was clearly observed in the band around 760 nm, which allowed us to correctly measure the fluorescence excitation spectrum.

Changes in the fluorescence spectrum upon the addition of increasing concentration of octenidine are shown in Fig. 4. The spectrum shifts to the short-wavelength region, and the integral intensity of the luminescence increases with an increase in the concentration of the antiseptic. The inset in Fig. 4 depicts the dependence of the position of the fluorescence maximum and the degree of increase in the fluorescence quantum yield, determined from the ratio of the areas under the fluorescence curve at various concentrations of octenidine. Note that the fluorescence intensity increases up to a maximum concentration of 300 μM , and then the fluorescence intensity decreases. At high concentrations of octenidine ($\geq 300 \mu\text{M}$), as in the case of picloxadine and chlordexidine, some Chl *a* molecules can be destroyed with a subsequent decrease in the fluorescence intensity (see Fig. 1).

As mentioned above, the main fluorescence band in PSII preparations consists of at least two spectral components detected at low-temperature measurements. The results presented in Fig. 4 indicate that under the influence of the antiseptic, the intensity of the luminescence of the long-wave component (the maximum at 690 nm) is greatly decreased. As a result, the fluorescence spectrum shifts to the short-wavelength region, while the intensity of the integral luminescence of the samples increases strongly in parallel with the shift of its maximum from 682 to 677 nm (Fig. 4, inset). CP43 and CP47 subunits contain chlorophylls that absorb at longer wavelengths than the RC chlorophylls. Moreover, according to Andrizhiyevskaya et al. (2005), the short-wavelength part of the fluorescence spectrum of PSII core complexes reflects the deactivation of excited states, the energy

Fig. 5 Changes in the fluorescence spectrum and its integrated intensity (inset) upon addition of Triton X-100 to PSII suspension at concentrations of 0.02, 0.05, 0.08, 0.1, 0.2, and 0.3%. The spectrum of the control preparation is shown by black curve. The arrow shows the direction of change in the fluorescence spectrum derived from the control spectrum in the presence of various concentrations of Triton X-100

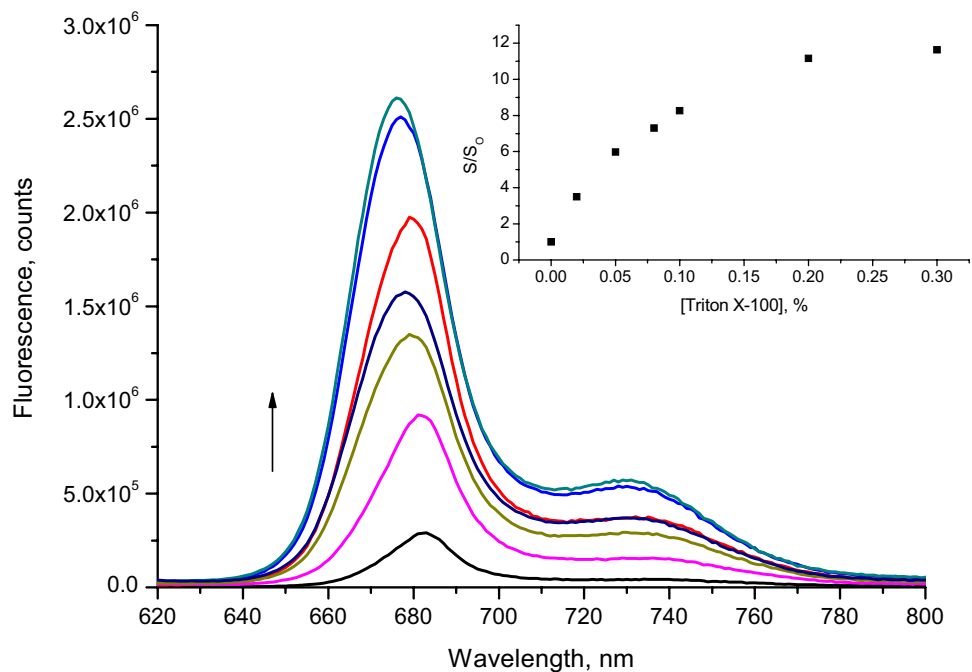


Table 1 The fluorescence lifetimes (τ_i) and amplitudes (a_i) for PSII core complexes at different concentrations of octenidine, Triton X-100, and after acetone treatment

	Control without ferricyanide	Control with ferricyanide	Octeni-dine 5 μ M	Octeni-dine 10 μ M	Octeni-dine 25 μ M	Octeni-dine 50 μ M	Octeni-dine 100 μ M	Octeni-dine 200 μ M	Triton 0.02%	Triton 1%	Acetone
τ_1 , ps	198 \pm 9	113 \pm 6	128 \pm 5	124 \pm 6	270 \pm 10	284 \pm 11	333 \pm 15	357 \pm 14	527 \pm 19		
τ_2 , ns	0.63 \pm 0.05	0.37 \pm 0.04	0.38 \pm 0.04	0.39 \pm 0.05	1.31 \pm 0.05	2.07 \pm 0.06	2.24 \pm 0.09	2.28 \pm 0.11	3.93 \pm 0.12		
τ_3 , ns	2.05 \pm 0.08	1.69 \pm 0.06	1.92 \pm 0.07	2.30 \pm 0.1	4.46 \pm 0.12	4.92 \pm 0.09	5.28 \pm 0.11	6.19 \pm 0.17		5.42 \pm 0.13	6.25 \pm 0.18
a_1 , %	80 \pm 3	85 \pm 5	82 \pm 4	80 \pm 5	65 \pm 4	59 \pm 5	58 \pm 4	57 \pm 5	32 \pm 4		
a_2 , %	14 \pm 2	14 \pm 3	17 \pm 4	17 \pm 4	21 \pm 5	31 \pm 4	32 \pm 4	33 \pm 3	68 \pm 6		
a_3 , %	6 \pm 2	1 \pm 0.4	1 \pm 0.4	3 \pm 0.6	14 \pm 3	10 \pm 2	10 \pm 2	10 \pm 3		100 \pm 10	100 \pm 10

λ_{ex} = 400 nm, λ_{em} = 680 nm. Control—without and in the presence of 350 μ M ferricyanide

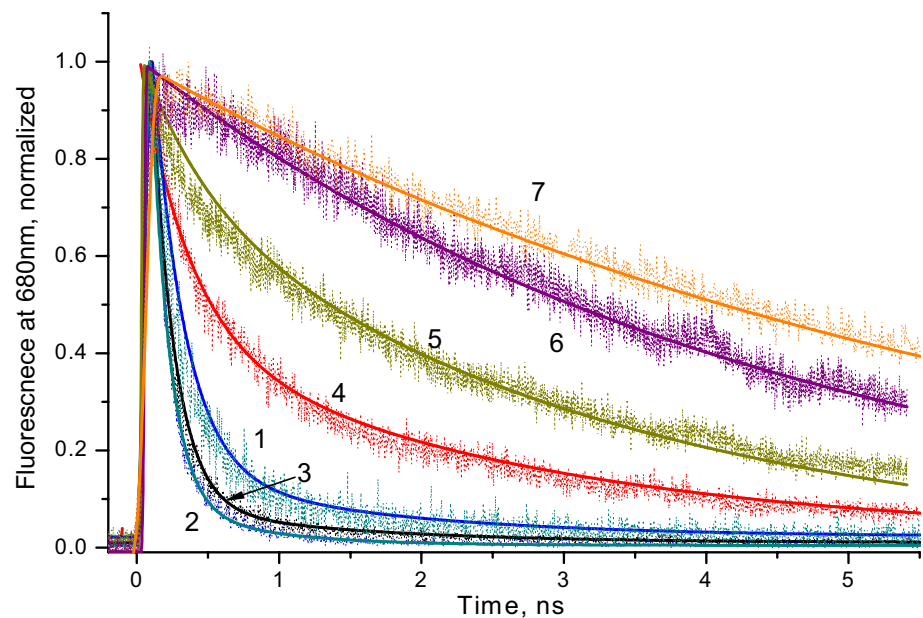
*The table shows the mean value for the three measurements and the standard error

of which is more slowly transferred to the reaction centers. Based on the data shown in Fig. 4, the effect of the antiseptic may be related to a change in the energy of Chl-protein interactions of some forms of Chl *a* in the light-harvesting antenna (CP43 and CP47), through which the excitation energy is delivered to the RC. It is known that the Chl molecules of these traps are the most remote (more than 20 Å) from the photoactive pigment P in the RC (Loll et al. 2005). The average time of the excitation energy delivery from the antenna into the RC is \sim 20 ps, while the average time of energy exchange between chlorophylls within the CP43 and CP47 complexes occur at a scale of 8 ps (van der Weij-de Wit et al. 2011).

Figure 5 depicts that adding detergent leads to an increase in the fluorescence intensity of the preparations and a shift of the maximum of the fluorescence band toward the short-wavelength region. Note that the similarity of the effect of Triton X-100 and octenidine on the fluorescence spectra of the PSII core complex is obvious. The dependence of the increase in the integral value of the fluorescence of PSII core complexes on the concentration of Triton X-100 is shown in the inset of Fig. 5.

The results of measuring the fluorescence kinetics in (i) PSII preparations in the absence and presence of potassium ferricyanide (350 μ M), as well as (ii) samples containing ferricyanide, followed by the addition of octenidine or Triton X-100 at various concentrations, are shown in Table 1. This table also includes the values of fluorescence lifetime of the acetone extract of the studied preparations. Figure 6 depicts some specific fluorescence decay kinetics and their approximation (solid curves). Note that potassium ferricyanide was used as an exogenous electron acceptor to assess the degree of reduction of the photoactive Chl of the RC upon activation of photoreactions by light pulses with a frequency of 80 MHz. The reduction of the photooxidized RC pigment in oxygen-evolving PSII core particles used by us occurs in \sim 30 ns (Haag et al. 1990). Taking into account that the time between activating light flashes is 12.5 ns, it can be expected that some of the RC complexes go into an inactive state during the time of recording the kinetics. Adding potassium ferricyanide resulted in the decrease in the fluorescence lifetime (curves 1 and 2 in Fig. 6 and the approximation data in the table). In the three-exponential approximation, at high concentrations of octenidine, a component with a duration of about 6 ns is correlated with the lifetime of free Chl in acetone (6.2 ns) or disintegrated pigment-protein complexes in the presence of Triton X-100 (5.4 ns). At the same time, in the presence of octenidine, a significant contribution ($a_1 = 57\%$) from the fast component is still preserved, which slows down by \sim 3 times compared to the control. In the presence of detergent and acetone, the decay kinetics becomes monoexponential.

Fig. 6 Fluorescence decay kinetics of PSII core complexes. 1—control sample without potassium ferricyanide; 2—control sample in the presence of 350 μM ferricyanide; 3—in the presence of 10 μM octenidine and 350 μM K ferricyanide; 4—in the presence of 100 μM octenidine and 350 μM K ferricyanide; 5—in the presence of 0.02% (w/v) Triton X-100; 6—in the presence of 1% Triton X-100; 7—in the presence of 80% acetone. $\lambda_{\text{ex}} = 400 \text{ nm}$, $\lambda_{\text{reg}} = 680 \text{ nm}$



Discussion

The results obtained in this work indicate the effect of the antiseptic octenidine on the PSII light-harvesting antenna complex. Based on the results obtained by several authors (de Paula et al. 1994; Neupane et al. 2010) we have proposed that the presence of an antiseptic leads to destabilization of chlorophylls in this structure and changes in their optical and functional characteristics. The high sensitivity of the PSII light-harvesting pigments to the state of the macromolecular carrier was mentioned above (see Introduction).

The significantly more pronounced effect of octenidine, in comparison with other antiseptics studied by us, is obviously associated with structural differences. Octenidine [N,N'-(1,10 decanediyldi-1[4H]-pyridinyl-4-ylidene)-bis-(1-octanamine) dihydrochloride] belongs to the group of bispyridines, where the aminopyridine structure enables a mesomeric distribution of the cationic charge. The two cationic pyridine residues are separated by ten methylene groups and each aminopyridine has a terminal hydrophobic octanyl group. In other words, the molecule is characterized by a pronounced amphipathic character, which allows it to be soluble in water and at the same time interact with hydrophobic cell membranes, up to destruction of their structure (Malanovic et al. 2020).

The mechanism of penetration of octenidine through various biomembranes may have common features. This could provide octenidine with the possibility of influencing the most diverse biological structures of living organisms of various systematic groups. In this regard, the results of the work (Malanovic et al. 2020) are indicative, where in a large complex study the detailed mechanism of the damaging effect of octenidine on gram-negative bacteria

(the majority of photosynthetic bacteria belong to them) was studied. In their work, the authors used a number of modern biophysical methods that made it possible to study the effect of octenidine on cell morphology.

According to the results of Malanovic et al. (2020), octenidine, with its positive charges, neutralizes the surface charge of the outer membrane of the bacterial cell. Because of hydrophobic interactions, the hydrocarbon chains from octenidine interfere with the fatty acyl chain region of the outer membrane core, inducing a complete lipid disorder based on hydrophobic mismatch. Additional octenidine molecules are able to penetrate from the outside through the periplasmic space to the inner membrane. As a result, the introduction of octenidine into the outer and inner membranes of bacteria leads to a chaotic arrangement of lipids and the rapid destruction of the cell membrane. The loss of membrane integrity is manifested in changes in their fluidity and it is also shown using electron microscopy. The destruction of the normal structure of the model membrane upon interaction with octenidine was also demonstrated by the molecular dynamics method in the works (Kholina et al. 2020; Rzycki et al. 2021). The membranes of plant cells, chloroplasts differ in their lipid composition from the membranes of bacterial cells. But they also contain negatively charged and neutral lipids (see, for example, a review by Reszczyńska and Hanaka (2020)). Thus, in particular, in spinach chloroplast membranes, negatively charged phosphoglycerol and sulfolipids make up about 20% (Reszczyńska and Hanaka 2020). In other words, octenidine molecules, which have pronounced amphipathic properties, are likely to be able to interact with both the negatively charged surface of plant membranes and their hydrophobic acyl tails.

The study of the effect of antiseptics on the structure of the model membrane by the method of molecular dynamics suggests that octenidine has the greatest destructive effect on the membrane. It significantly increased the area occupied by lipids in the membrane, "pushing" the acyl tails of the molecules (Kholina et al. 2020; Rzycki et al. 2021). In this regard, the target of antiseptic molecules penetrating into the PSII protein can probably also be the fraction of numerous lipid molecules in the structure of the core complex. According to Sheng et al. (2018), each monomer of the homodimeric system of such a complex includes 34 well-defined lipid molecules, which are essential for the interaction of core subunits. Thus, octenidine can obviously serve as an effective agent that destabilizes the initial state of the photosynthetic pigment-protein complex.

The fluorescence decay kinetics of PSII core complexes under various treatments is shown in Fig. 6; the approximation parameters in the three-exponential fitting are given in the Table 1. In the absence of ferricyanide, as an exogenous electron acceptor of the PSII RCs, the lifetime of the fast component is $\tau_1 \approx 200$ ps. This is a rather large value of the τ_1 component, usually associated with the process of energy migration from the core antenna to the RC. The reason for such a large value of τ_1 may be either the structural features of the preparations used in this work or partial closure of the RC under the action of high-frequency pulses of exciting light. Adding ferricyanide leads to a significant decrease in τ_1 to 113 ps. This clearly shows that in the control (original) samples, at least part of the RC was closed. The obtained value $\tau_1 = 113$ ps also exceeds the value of 50–80 ps reported in (Haehnel et al. 1983; van der Weij-de Wit et al. 2011). This can be explained either by the structural features of our sample or incomplete reduction of the RC even in the presence of 350 μM ferricyanide. Subsequently, the preparation containing 350 μM ferricyanide was considered as a control sample in our experiments.

Figure 6 and Table 1 shows that with an increase in the concentration of octenidine, the lifetime of the τ_1 component increases, reaching a value of 357 ps at 200 μM . Such a three-fold slowdown in the energy migration rate is accompanied by a 6–eightfold increase in the fluorescence intensity (Figs. 1 and 4). The increase in the fluorescence intensity is explained by a significant redistribution of amplitudes (a_i) of the three components of the decay kinetics and an increase in the lifetime (τ_i) of all components. We assume that such an effect of octenidine on the PSII core complexes is due to damaging of the native structure of the protein complex, as in the case of samples treated by detergent Triton X-100; in doing so, we cannot accurately localize the specific sites of action of an antiseptic that has both hydrophilic and hydrophobic properties. However, as can be seen from Fig. 3, the addition of octenidine leads to some decrease in the

optical density of the sample, a shift in the position of the long-wavelength maximum Q_y of the absorption band and changes in the blue-green part of the absorption spectrum. A decrease in extinction in the region of 420–500 nm indicates pheophytinization of some part of antenna Chl molecules (Wang et al. 2020).

Purified PSII core complexes are very sensitive to isolation procedures (de Paula et al. 1994). Structural factors, such as the distance between the energy donor and acceptor, molecular orientation, and vibronic interactions, can either promote or hinder efficient energy transfer and charge separation in PSII. Thus, the isolated protein-pigment complexes can contain (i) PSII fractions in which efficient energy transfer and effective stabilization of photoseparated charges are preserved (fluorescence lifetime, $\tau \sim 0.1$ ns), (ii) complexes with impaired energy transfer and stabilization of photoseparated charges (fluorescence lifetime, $\tau \sim 1$ ns), and (iii) complexes with destroyed Chl–Chl and Chl–protein interactions (fluorescence lifetime, τ , more than 5 ns). Note that the incubation medium for the solubilized complexes makes an important contribution to this heterogeneity. In fact, de Paula et al. (1994) showed that the fast fluorescence component with $\tau \sim 0.1$ ns completely disappears, while the component with $\tau \sim 6$ ns becomes dominant in isolated PSII RC and RC-CP47 complexes treated by Triton X-100 (0.2% w/v). Similar data were obtained in the present work (Table 1).

When approximating the experimental fluorescence decay kinetics (Fig. 6), we used the three-exponential fitting, which gives the smallest value of the standard deviation χ^2 . The presence of three components in the PSII fluorescence decay kinetics in the ranges of about one hundred ps, components with characteristic times of several hundred ps and more has also been reported (Hansson et al. 1988; De Paula et al. 1994). At the same time, the appearance and elongation of slow components is due to the appearance of closed PSII RCs (Haehnel et al. 1983; Karukstis and Sauer 1984; Moya et al. 1986; Hodges and Moya 1988; Keuper and Sauer 1989). Some data indicates the presence of four (Andrizhiyevskaya et al. 2004) or even five components (van der Weij-de Wit et al. 2011). It has been suggested that the registered components of picosecond and even subpicosecond duration are probably related to the energy equilibration within the CP43 and CP47 subunits. Thus, we assume that the three-component representation of the fluorescence decay kinetics of PSII core complexes is justified if the process of excitation equalization in the PSII core antenna complexes, CP43 and CP47, is not taken into account. Finally, we attributed the second component of average lifetime to the process of charge recombination in RCs. Its magnitude in control samples with ferricyanide is $\tau_2 = 0.37$ ns, which is close to the value of 360–460 ps (Andrizhiyevskaya et al. 2004). As can be seen from Table 1 upon addition of octenidine the value of τ_2 increases to

2.28 ns, and the amplitude increases from $14 \pm 2\%$ to $33 \pm 3\%$. These values are in good agreement with the results obtained by van Mieghem and his co-workers (1992). In doing so, both in PSII-enriched photosynthetic membranes and in PSII core complexes in the presence of dithionite, leading to the appearance of doubly reduced Q_A , the dominant fluorescence component ($\sim 70\%$), as in the case of samples with oxidized Q_A , is characterized by $\tau \sim 200$ ps. This component should be assigned to τ_1 , which we revealed in the present work. At the same time, under conditions of singly reduced Q_A , the fastest fluorescence component had $\tau \sim 600$ ps (25%), while the other two components were characterized by $\tau \sim 1.4$ ns (68%) and $\tau \sim 3.3$ ns (7%). It has been suggested that the fastest kinetic phase (200 ps) reflects the high efficiency of charge separation in the RC due to the absence of an electric charge on Q_A (Mieghem et al. 1992). This is explained by the double protonation of doubly reduced Q_A . Note that we also obtained τ_2 values close to those reported in (Mieghem et al. 1992) for PSII core complexes with singly reduced Q_A at various concentrations of octenidine. Apparently, as the concentration of octenidine increases, the efficiency of photochemical conversion of light energy in the RCs decreases, which leads to an increase in the probability of a reverse reaction of energy transfer from the RCs to the antenna complex. In parallel with this process, the proportion of oxidized RCs increases, which is accompanied by a successive increase in the values of τ_2 and a_2 (Table 1).

Our previous investigation (Strakhovskaya et al. 2021; Knox et al. 2022) focused on the effect of various antiseptics on the spectral characteristics and energy migration processes in the chromatophores isolated from non-sulfur purple bacteria *Rba. sphaeroides* and *R. rubrum*. The addition of octenidine to chromatophore vesicles resulted in an approximately threefold decrease in the efficiency of electron excitation energy migration from antenna complexes LH2 to LH1-RC (*Rba. sphaeroides*) and a twofold decrease in the rate of energy migration from LH1 to the RC in *R. rubrum*. At the same time, the fluorescence intensity in *R. rubrum* chromatophores increased 5.5–6.6 times. It was concluded that octenidine increased the intramolecular fluorescence rate constant as a result of a change in the polarity of the microenvironment of BChl molecules included in the LH1 complex of *R. rubrum* and in the LH2 complex of *Rba. sphaeroides*. Note that adding octenidine leads to the appearance of free molecules of bacteriopheophytin and bacteriochlorophyll (Strakhovskaya et al. 2021; Knox et al. 2022).

The addition of octenidine to PSII core complexes rather leads to a destructive effect on the pigment-protein structure of the complex, as in the case of Triton-treated samples. As a result, the duration of the τ_2 component strongly increases, which is probably related to the light-induced recombination

of the radical ion pair. In doing so, we attribute the τ_3 component to fragments with impaired Chl–Chl and Chl–protein interactions. Simultaneously with an increase in the duration's τ_2 and τ_3 , a significant increase in the amplitudes a_2 and a_3 of these components is also observed. In the case of PSII core complexes, there are no reliable grounds to assume a change in the intramolecular deactivation rate constant k_{fl} in light-harvesting Chl molecules for samples treated with octenidine. This is most likely due to the effect of this compound on the structural elements of the PSII core complex.

We also investigated the effect of octenidine on the steady-state oxygen-evolving activity in PSII core particles. The rate of oxygen evolution decreased from 1500 (in control sample) up to 560 and 230 $\mu\text{mol O}_2 \cdot (\text{mg Chl} \cdot \text{h})^{-1}$ in the presence of 50 μM and 100 μM octenidine, respectively (data not shown).

Conclusion

Among the preparations of photosynthetic organisms studied by us, the greatest effect of the antiseptic octenidine on the spectral properties and processes of energy migration was found in *Rba. sphaeroides* and *R. rubrum* chromatophores (Strakhovskaya et al. 2021; Knox et al. 2022), as well as in PSII core complexes (this work). This agent, produced by Shulke and Mayr (Germany), has an extremely high biocidal activity, affecting the structure of the bacterial cell walls and pathogens cell membranes. As a result of this exposure, pathogens die. The biocidal activity of octenidine significantly exceeds the activity of miramistin, chlorhexidine, and other known antiseptics (Assadian 2016). It becomes evident that when interacting with the components of the membranes of photosynthetic organisms, octenidine disrupts the structure of protein complexes, the efficiency of interaction between the components of the complexes, as well as between Chl (Bchl) molecules and protein. In addition, under the influence of even low concentrations of octenidine, some Chl (Bchl) molecules can lose the central Mg atom and transform into another form of porphyrins, Pheo (Bpheo). In addition, the antiseptic effect is manifested in a change in the absorption and fluorescence spectra, as well as the efficiency of photochemical conversion of the light energy. The most striking manifestation of the effect of octenidine on the chromatophores and PSII core complexes was an increase in the integrated fluorescence intensity by 5–10 times. We explained this effect in the case of chromatophores by a decrease in the rate constant of energy migration from LH2 to LH1 (*Rba. sphaeroides*) and from LH1 to the RC (*R. rubrum*), as well as by a change in the polarity of the microenvironment of BChl molecules in light-harvesting complexes. According to our estimates, the number of monomeric BChl and Bpheo molecules that

appeared under the action of octenidine was insignificant. In the case of PSII core complexes, the main effect of octenidine is probably associated with structural alterations in the complexes. This can also be evidenced by data on the effect of octenidine on the steady-state rate of oxygen evolution. Adding this antiseptic at a concentration of 100 μM decreased the oxygen-evolving activity by about 85% compared to the control. In fact, the action of octenidine and Triton X-100 was very similar. However, it cannot be ruled out that a change in polarity in the environment of Chl molecules can lead to an increase in the fluorescence intensity. The latter can occur due to an increase in the intramolecular fluorescence rate constant.

The effect of octenidine on the processes of conversion of light energy by the components of the photosynthetic apparatus indicates that this agent should be used in large quantities with some caution. In doing so, the consequences of its widespread use for antiseptic purposes can have a negative impact on the environment. It should be noted that spinach PSII is an evolutionary homologue of the photosynthetic apparatus of purple photosynthetic bacteria. It is also an integral part in the photosynthetic apparatus of oxygen-producing cyanobacteria, algae [precursors of chloroplasts] (Raymond and Blankenship 2004). Thus, the massive ingress of antiseptics into the water resources of the planet can have significant negative consequences for both aquatic- and terrestrial photosynthetic organisms. In this regard, it may become relevant to monitor the state of PSII in aquatic organisms for environmental contamination with antiseptics. One of the methods for such monitoring, for example, is remote analysis of fluorescence induction, which reflects the lifetime state of PSII in aqueous photosynthetic organisms (Voronova et al. 2019).

Acknowledgements Funding the research was carried out as a part of the Science Project of the State Order of the Government of Russian Federation to Lomonosov Moscow State University N 121,032,500,058–7.

Declarations

Conflict of interest The authors declare no conflicts of interest.

Data Availability Not applicable.

Code Availability Not applicable.

References

- Andrizhiyevskaya EG, Frolov D, van Grondelle R, Dekker JP (2004) On the role of the CP47 core antenna in the energy transfer and trapping dynamics of Photosystem II. *Phys Chem Chem Phys* 6:4810–4819
- Andrizhiyevskaya EG, Chojnicka A, Bautista JA, Diner BA, van Grondelle R, Dekker JP (2005) Origin of the F685 and F695 fluorescence in Photosystem II. *Photosynth Res* 84:173–218
- Assadian O (2016) Octenidine dihydrochloride: chemical characteristics and antimicrobial properties. *J Wound Care* 25(Sup3):S3–S6. <https://doi.org/10.12968/jowc.2016.25.Sup3.S3>
- de Paula JC, Liefshitz A, Hinsley S, Lin W, Chopra V, Long K, Williams SA, Belts S, Yocum CF (1994) Structure-function relationships in the 47-kDa antenna protein and its complex with the photosystem II reaction center core: insights from picosecond fluorescence decay kinetics and resonance Raman spectroscopy. *Biochemistry* 33:1455–1466
- French CS, Smith JHC, Virgin HI, Airth RL (1956) Fluorescence-spectrum curves of chlorophylls, pheophytins, phycoerythrins, phycocyanins and hypericin. *Plant Physiol* 31:369–374
- Groot M-L, Peterman EJG, Van Stokkum IHM, Dekker JP, van Grondelle R (1995) Triplet and fluorescing states of the CP47 antenna complex of photosystem II studied as a function of temperature. *Biophys J* 68:281–290
- Groot M-L, Frese RN, de Weerd FL, Bromek K, Pettersson A, Peterman EJG, van Stokkum IHM, van Grondelle R, Dekker JP (1999) Spectroscopic properties of the CP43 core antenna protein of photosystem II. *Biophys J* 77:3328–3340
- Guskov A, Kern J, Gabdulkhakov A, Broser M, Zouni A, Saenger W (2009) Cyanobacterial photosystem II at 2.9-Å resolution and the role of quinones, lipids, channels and chloride. *Nature Struct Mol Biol* 16:334–342
- Haag E, Irrgang KD, Boekema EJ, Renger G (1990) Functional and structural analysis of photosystem II core complexes from spinach with high oxygen evolution capacity. *Eur J Biochem* 189:47–53
- Haehnel W, Holzwarth AR, Wendler J (1983) Picosecond fluorescence kinetics and energy transfer in the antenna chlorophylls of green algae. *Photochem Photobiol* 37:435–443
- Hansson O, Durantion J, Mathis P (1988) Yield and lifetime of the primary radical pair in preparations of Photosystem II with different antenna size. *Biochim Biophys Acta* 932:91–96
- Hodges M, Moya I (1988) Time-resolved chlorophyll fluorescence studies on pigment-protein complexes from photosynthetic membranes. *Biochim Biophys Acta* 935:41–52
- Karukstis KK, Sauer K (1984) Organization of the photosynthetic apparatus of the *chlorina-f2* mutant of barley using chlorophyll fluorescence decay kinetics. *Biochim Biophys Acta Bioenergetics* 766:148–155
- Kern J, Renger G (2007) Photosystem II: structure and mechanism of the water: plastoquinone oxidoreductase. *Photosynth Res* 94(2–3):183–202
- Keuper HJK, Sauer K (1989) Effect of photosystem II reaction center closure on nanosecond fluorescence relaxation kinetics. *Photosynth Res* 20:85–103
- Kholina EG, Kovalenko IB, Bozdaganyan ME, Strakhovskaya MG, Orekhov PS (2020) Cationic antiseptics facilitate pore formation in model bacterial membranes. *J Phys Chem B* 124:8593–8600
- Knox PP, Lukashev EP, Korvatovskiy BN, Strakhovskaya MG, Makhneva ZK, Bol'shakov MA, Paschenko VZ (2022) Disproportionate effect of cationic antiseptics on the quantum yield and fluorescence lifetime of bacteriochlorophyll molecules in the LH1-RC complex of *R. rubrum* chromatophores. *Photosynth Res*. <https://doi.org/10.1007/s11120-022-00909-8>
- Loll B, Kern J, Saenger W, Zouni A, Biesiadka J (2005) Towards complete cofactor arrangement in the 3.0 angstrom resolution structure of photosystem II. *Nature* 438:1040–1044
- Lubitz W, Chrysina M, Cox N (2019) Water oxidation in photosystem II. *Photosynth Res* 142(1):105–125
- Malanovic N, Ön A, Pabst G, Zellner A, Lohner K (2020) Octenidine: novel insights into the detailed killing mechanism of

- Gram-negative bacteria at a cellular and molecular level. *Intern J Antimicrob Agents* 56:106146
- Moya I, Hodges M, Barbet J-C (1986) Modification of room-temperature picosecond chlorophyll fluorescence kinetics in green algae by photosystem II trap closure. *FEBS Lett* 198:256–262
- Neupane B, Dang NC, Acharya K, Reppert M, Zazubovich V, Picorel R, Seibert M, Jankowiak R (2010) Insight into the electronic structure of the CP47 antenna protein complex of photosystem II: hole burning and fluorescence study. *J Am Chem Soc* 132:4214–4229
- Porra RJ, Thompson WA, Kriedemann PE (1989) Determination of accurate extinction coefficients and simultaneous equations for assaying chlorophylls a and b extracted with four different solvents: verification of the concentration of chlorophyll standards by atomic absorption spectroscopy. *Biochim Biophys Acta* 975:384–394
- Raymond J, Blankenship RE (2004) The evolutionary development of the protein complement of Photosystem 2. *Biochim Biophys Acta* 1655:133–139
- Reszczyńska E, Hanaka A (2020) Lipids composition in plant membranes. *Cell Biochem Biophys* 78:401–414
- Rzycki M, Drabik D, Szostak-Paluch K, Hanus-Lorenz B, Kraszewski S (2021) Unraveling the mechanism of octenidine and chlorhexidine on membranes: does electrostatics matter? *Biophys J* 120:3392–3408
- Schatz GH, Brock H, Holzwarth AR (1988) Kinetic and energetic model for the primary processes in photosystem II. *Biophys J* 54:397–405
- Shan J, Wang J, Ruan X, Li L, Gong Y, Zhao N, Kuang T (2001) Changes of absorption spectra during heat-induced denaturation of Photosystem II core antenna complexes CP43 and CP47: revealing the binding states of chlorophyll molecules in these two complexes. *Biochim Biophys Acta* 1504:396–408
- Sheng X, Liu X, Cao P, Li M, Liu Z (2018) Structural roles of lipid molecules in the assembly of plant PSII-LHCII supercomplex. *Biophys Rep* 4:189–203
- Shibata Y, Nishi S, Kawakami K, Shen J-R, Renger T (2013) Photosystem II does not possess a simple excitation energy funnel: time-resolved fluorescence spectroscopy meets theory. *J Am Chem Soc* 135:6903–6914
- Strakhovskaya MG, Lukashev EP, Korvatovskiy BN, Kholina EG, Seifullina NK, Knox PP, Paschenko VZ (2021) The effect of some antiseptic drugs on the energy transfer in chromatophore photosynthetic membranes of purple non-sulfur bacteria *Rhodospira rubra*. *Photosynth Res* 147:197–209
- Suga M, Akita F, Hirata K, Ueno G, Murakami H, Nakajima Y, Shimizu T, Yamashita K, Yamamoto M, Ago H, Shen J-R (2015) Native structure of photosystem II at 1.95 Å resolution viewed by femtosecond X-ray pulses. *Nature* 517:99–103
- Umehara Y, Kawakami K, Shen JR, Kamiya N (2011) Crystal structure of oxygen-evolving photosystem II at a resolution of 1.9 Å. *Nature* 473:55–65
- van Mieghem FJE, Searle GFW, Rutherford AW, Schaafsma TJ (1992) The influence of the double reduction of OA on the fluorescence decay kinetics of Photosystem II. *Biochim Biophys Acta* 1100:198–206
- van der Weij-de Wit CD, Dekker JP, van Grondelle R, van Stokkum IHM (2011) Charge separation is virtually irreversible in photosystem II core complexes with oxidized primary quinone acceptor. *J Phys Chem A* 11:3947–3956
- Voronova EN, Konyukhov IV, Koksharova OA, Popova AA, Pogoyan SI, Khmel IA, Rubin AB (2019) Inhibition of cyanobacterial photosynthetic activity by natural ketones. *J Phycol* 55:840–857
- Wang L, Jiang L, Xing X, Chen Y, Meng Q (2020) The effects of phytytin a on absorption properties of phytoplankton in Dalian Bay, China. In: 7th Annual International Conference on Geo-Spatial Knowledge and Intelligence IOP Conference Series: Earth and Environmental Science, vol. 428. IOP Publishing, p 012048. <https://doi.org/10.1088/1755-1315/428/1/012048>
- Wei X, Su X, Cao P et al (2016) Structure of spinach photosystem II-LHCII supercomplex at 3.2 Å resolution. *Nature* 534:69–74
- Wydrzynski T, Satoh K (2005) Photosystem II: the light-driven water-plastoquinone oxidoreductase. Springer, Amsterdam

Publisher's Note Springer Nature remains neutral with regard to jurisdictional claims in published maps and institutional affiliations.

Springer Nature or its licensor (e.g. a society or other partner) holds exclusive rights to this article under a publishing agreement with the author(s) or other rightsholder(s); author self-archiving of the accepted manuscript version of this article is solely governed by the terms of such publishing agreement and applicable law.